Selection of Optimal Operating Conditions for a Continuous CO2–Capture Process Using an Aqueous Ammonia Solution

6 AUTHORS, INCLUDING:

Kwang Bok Yi
Chungnam National University
46 PUBLICATIONS **622** CITATIONS

SEE PROFILE

Chang Hyun Ko
Chonnam National University
83 PUBLICATIONS **2,302** CITATIONS

SEE PROFILE

Jong-Nam Kim
Korea Institute of Energy Research
61 PUBLICATIONS **901** CITATIONS

SEE PROFILE

Won Hi Hong
Korea Advanced Institute of Science and Tec…
170 PUBLICATIONS **3,983** CITATIONS

SEE PROFILE

energy&fuels
article

Selection of Optimal Operating Conditions for a Continuous CO_2-Capture Process Using an Aqueous Ammonia Solution

Sung Youl Park,[†,‡] Kwang Bok Yi,[†] Chang Hyun Ko,[†] Jong-Ho Park,[†] Jong-Nam Kim,*[,†] and Won Hi Hong*[,‡]

[†]*Greenhouse Gas Research Center, Korea Institute of Energy Research, 71-2 Jang-dong, Yuseong-gu, Daejeon, Republic of Korea, and* [‡]*Department of Chemical and Biomolecular Engineering, Korea Advanced Institute of Science and Technology, 373-1 Guseong-dong, Yuseong-gu, Daejeon, Republic of Korea*

Received March 11, 2010. Revised Manuscript Received May 4, 2010

The optimal conditions of the absorbent concentration, rich CO_2 loading, and regeneration temperature in a continuous CO_2-capture process using a 3−27 wt % aqueous NH_3 solution were experimentally studied and compared to vapor−liquid equilibrium of a CO_2−NH_3−H_2O system. The dependence of CO_2 removal efficiency upon the NH_3 concentration and regeneration temperature was well-explained by the regeneration critical condition, which was defined using mole fractions of CO_2, NH_3, and H_2O in the vapor phase at equilibrium. The optimal conditions were 12 wt % NH_3 concentration, 0.36 rich CO_2 loading, and a 90 °C regeneration temperature. Use of the vapor−liquid equilibrium data of the CO_2−NH_3−H_2O system at regeneration conditions can be employed as a method to select the optimal operating conditions of a regeneration system and can provide guidelines for the design and operation of a CO_2-capture process using aqueous NH_3 solution.

1. Introduction

As global warming has become one of the most pressing issues globally, a considerable body of related research has focused on CO_2-capture technologies. Chemical absorption is known to be the most promising approach for the separation method of CO_2 from gas mixtures having a low partial pressure of CO_2, such as flue gas, and various studies in this area have been carried out. The most commonly used absorbents for CO_2 capture are aqueous solutions of alkanolamines, such as monoethanolamine (MEA), diethanolamine (DEA), diisopropanolamine (DIPA), and methyldiethanolamine (MDEA),[1,2] and these single alkanolamines are competing with sterically hindered amines, such as 2-amino-2-methyl-1-propanol (AMP).[3,4] Blends of alkanolamines and sterically hindered amines have also been widely studied, yielding data on solubility, mass transfer, and reaction kinetics.[5,6]

Alternative processes using aqueous ammonia (NH_3) solution are known to offer notable advantages over conventional amine-based CO_2-capture technologies, and research on CO_2 capture has been actively conducted.[7−11] Equilibrium in the CO_2−NH_3−H_2O system has been widely studied. Vapor−liquid−solid (VLS) equilibrium of the CO_2−NH_3−H_2O system at 310−470 K was studied and thermodynamically modeled using a thermodynamic framework.[12] An optimization method for modeling the solubility of CO_2 and NH_3 in H_2O was studied in a temperature range of 333−473 K and at NH_3 concentrations below 13 M. The solubility data were correlated using the Pitzer model, and the interaction parameters were identified.[13] Studies of vapor−liquid equilibrium (VLE) in the CO_2−NH_3−H_2O system using a NH_3 concentration up to 16 M and CO_2 concentration up to 13 M at 333−393 K and 7 MPa were conducted.[14] On the basis of the research of the CO_2−NH_3−H_2O system, the absorption and regeneration of CO_2 in a semibatch reactor using 8 wt % aqueous ammonia solution were studied and it was shown that the CO_2 carrying capacity and regeneration energy of a 8 wt % aqueous ammonia solution were higher than those of a 20 wt % aqueous MEA solution.[7] Research on the reaction kinetics of CO_2 in an aqueous ammonia solution was carried out using various concentrations of aqueous ammonia solutions (0.07, 0.10, and 0.14 mol of NH_3/L) and CO_2 (10, 12, and 14 vol % CO_2).[15] Furthermore, various studies on the development of a commercial CO_2-capture process using aqueous NH_3 solution have been conducted,[16−21] although the detailed technologies, including

*To whom correspondence should be addressed. Fax: 82-42-860-3631. E-mail: jnkim@kier.re.kr (J.-N.K.); Fax: 82-42-350-3910. E-mail: whhong@kaist.ac.kr (W.H.H.).

(1) Chakma, A. *Energy Convers. Manage.* **1995,** *36* (6), 405–410.
(2) Al-Ghawas, H. A.; Hagewiesche, D. P.; Ruiz-lbanez, G.; Sandall, O. C. *J. Chem. Eng. Data* **1989,** *34* (4), 385–391.
(3) Saha, A.; Bandyopadhyay, S. *Chem. Eng. Sci.* **1995,** *50* (22), 3587–3598.
(4) Bosch, H.; Versteeg, G. F.; van Swaaij, W. P. M. *Chem. Eng. Sci.* **1990,** *45* (5), 1167–1173.
(5) Dey, A.; Aroonwilas, A. *Energy Procedia* **2009,** *1,* 211–215.
(6) Mandal, B. P.; Bandyopadhyay, S. S. *Chem. Eng. Sci.* **2006,** *61* (16), 5440–5447.
(7) Yeh, J. T.; Resnik, K. P.; Rygle, K.; Pennline, H. W. *Fuel Process. Technol.* **2005,** *86* (14−15), 1533–1546.
(8) Lee, J. W.; Li, R. *Energy Convers. Manage.* **2003,** *44* (9), 1535–1546.
(9) Huang, H.; Chang, S. G. *Energy Fuels* **2002,** *16* (4), 904–910.

(10) Yeh, A. C.; Bai, H. *Sci. Total Environ.* **1999,** *228,* 121–133.
(11) Hsunling, B.; An Chin, Y. *Ind. Eng. Chem. Res.* **1997,** *36* (6), 2490–2493.
(12) Kurz, F.; Rumpf, B.; Maurer, G. *Fluid Phase Equilib.* **1995,** *104,* 261–275.
(13) Biling, V.; Rumpf, B.; Strepp, F.; Maurer, G. *Fluid Phase Equilib.* **1989,** *53,* 251–259.
(14) Göppert, U.; Maurer, G. *Fluid Phase Equilib.* **1988,** *41* (1−2), 153–161.
(15) Diao, Y. F.; Zheng, X. Y.; He, B. S.; Chen, C. H.; Xu, X. C. *Energy Convers. Manage.* **2004,** *45* (13−14), 2283–2296.
(16) Darde, V.; Thomsen, K.; van Well, W. J. M.; Stenby, E. H. *Energy Procedia* **2009,** *1* (1), 1035–1042.
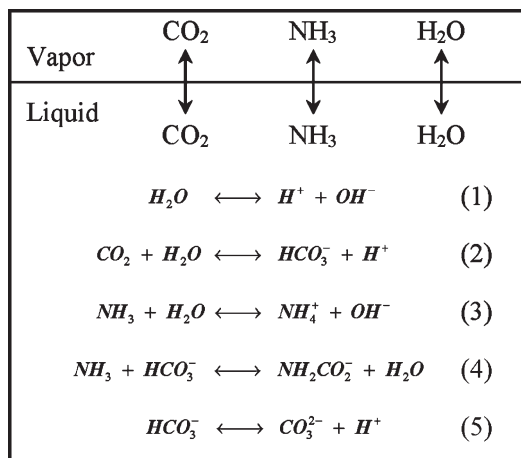
Vapor	CO_2	NH_3	H_2O
Liquid	CO_2	NH_3	H_2O

$$H_2O \longleftrightarrow H^+ + OH^- \qquad (1)$$

$$CO_2 + H_2O \longleftrightarrow HCO_3^- + H^+ \qquad (2)$$

$$NH_3 + H_2O \longleftrightarrow NH_4^+ + OH^- \qquad (3)$$

$$NH_3 + HCO_3^- \longleftrightarrow NH_2CO_2^- + H_2O \qquad (4)$$

$$HCO_3^- \longleftrightarrow CO_3^{2-} + H^+ \qquad (5)$$

Figure 1. Reactions of absorption and desorption in the CO_2–NH_3–H_2O system.[7,11,15,22]

operating conditions, have not been made public. It should be noted, however, that little research on continuous CO_2 capture using an aqueous ammonia solution has been reported.

The objective of this study is to suggest a method for the selection of optimal operating conditions, such as CO_2 loading of a rich absorbent, regeneration temperature, and NH_3 concentration of the absorbent, all of which are non-equipment-specific parameters. In this work, CO_2 removal efficiency is measured in a continuous lab-scale CO_2-capture process with various operating conditions, such as regeneration temperature and flow rates of feed gas and absorbent. The method is derived from a comparison of experimental results to a theoretical approach using mole fractions of CO_2, NH_3, and H_2O in the vapor phase at VLE.

2. Reactions in the CO_2–NH_3–H_2O System

The reactions that occur in absorption and desorption of CO_2 using an aqueous NH_3 solution can be described by the equations in Figure 1.

Absorption occurs through the dissolution of CO_2 in H_2O, and further reactions in the form of electrolytes in liquid and the desorption of CO_2 from liquid occur through reverse reactions of absorption. In a continuous operation, NH_3 in the liquid and vapor phase is in equilibrium according to the temperature of the absorption and desorption process.

3. Experimental Section

3.1. Experimental Apparatus. Continuous CO_2-capture experiments were conducted using a lab-scale experimental apparatus. A schematic diagram of the continuous ammonia-based CO_2-capture apparatus is shown in Figure 2.

The experimental apparatus consists of a CO_2 absorber, a stripper, washing columns, and a wash water regenerator. The CO_2 absorber is made of polymethyl methacrylate (PMMA), with a diameter of 50 mm and a height of 1 m. The absorption column was directly connected to a washing column, which is

made of PMMA, with a diameter of 50 mm and a height of 0.5 m. To measure the temperature profile along the CO_2 absorber height, 10 thermocouples were installed at 10 cm intervals. The CO_2 stripper is made of glass, with a diameter of 50 mm and a height of 0.5 m. It was also directly connected to a washing column, which is made of glass, with a diameter of 50 mm and a height of 0.3 m. The wash water regenerator is made of glass, with a diameter of 50 mm and a height of 0.3 m. All columns were packed with structured packing made of stainless-steel wire gauze (Sulzer BX). Reboilers for the CO_2 stripper and the wash water regenerator are made of stainless steel, and the temperatures were controlled by electric heaters immersed in liquid. The reboiler for the CO_2 stripper was operated in a range of 75−97 °C, and the reboiler for the wash water regenerator was operated at 100 °C.

3.2. Materials and Methods. The feed gas was prepared by mixing pure CO_2 and dry air. The concentration was adjusted to 10 vol % CO_2 by mass flow controllers (Brooks Instrument 5850E) and supplied to the absorber with flow rates of 1, 2, and 3 m^3/h at ambient temperature. The concentration of CO_2 in the gas stream was measured by a CO_2 gas analyzer (IR gas analyzer, Fuji Electronics). All used data were collected at a steady state of continuous operation. The removal efficiencies of CO_2 can be obtained from the following formula:

$$\eta_{CO_2} = \frac{(V_{CO_2,\,in} - V_{CO_2,\,out}) \times 100\%}{V_{CO_2,\,in}} \qquad (6)$$

where η_{CO_2} is the CO_2 removal efficiency and $V_{CO_2,in}$ and $V_{CO_2,out}$ are the inlet and outlet volume of CO_2, respectively. The concentrations of the absorbent were adjusted to 3, 6, 13, 20, and 27 wt % NH_3 by mixing a commercial-grade aqueous NH_3 solution (Samcheon, Korea) with distilled water, and the flow rates were controlled to 50, 100, 150, 200, and 250 mL/min at 20 °C. Wash water for washing columns above the absorber and the stripper were continuously circulated with a flow rate of 150 mL/min at 8 °C. The regenerated water was supplied to the circulation loops, which are located above the absorber and stripper, with flow rates of 50 and 100 mL/min at 8 °C, respectively. The same amount of wash water was separated from the circulation loop and fed to the wash water regenerator. The concentrations of NH_3 and CO_2 in liquids were measured by an acid−base titration method. All liquid samples of 10 mL were mixed with 20 mL of 1 N NaOH and 1 N $BaCl_2$ aqueous solution. The amounts of NH_3 and CO_2 in the liquid samples were calculated from the titration results (848 TitrinoPlus, Metrohm) using an aqueous solution of 1 N HCl at 2 °C. All chemicals used in the titration were reagent-grade (Sigma-Aldrich). The performance of a continuous CO_2-capture process depends upon the regeneration of rich absorbents. To identify the behaviors of regeneration, the mole fractions of CO_2 and NH_3 in the vapor phase were calculated using AspenPlus; ElectrolyteNRTL was used for the property method, and a flash process model was used for calculation of the VLE.

4. Results and Discussion

4.1. Effect of the Flow Rate and NH_3 Concentration. Figure 3a shows the effect of the NH_3 concentration on the removal efficiency. For all absorbent flow rates, the removal efficiency rapidly increases as the NH_3 concentration increases until 12 wt % and remains nearly constant above this concentration.

Figure 3b shows the effect of the absorbent flow rate on the removal efficiency. The removal efficiency increases as the absorbent flow rate increases. In the case of the NH_3 concentration above 12 wt %, the removal efficiency increases until 150 mL/min and shows a relatively slow increase above this flow rate. A similar change of the removal efficiency occurs between 150 and 200 mL/min when the NH_3 concentration is below 6 wt %. For all absorbent flow rates, the

(17) Kozak, F.; Petig, A.; Morris, E.; Rhudy, R.; Thimsen, D. *Energy Procedia* **2009**, *1* (1), 1419–1426.
(18) Valenti, G.; Bonalumi, D.; Macchi, E. *Energy Procedia* **2009**, *1* (1), 1059–1066.
(19) Koeijer, G.; Enge, Y. O.; Thebault, C.; Berg, S.; Lindland, J.; Overa, S. J. *Energy Procedia* **2009**, *1* (1), 1321–1326.
(20) Derks, P. W. J.; Versteeg, G. F. *Energy Procedia* **2009**, *1* (1), 1139–1146.
(21) Figueroa, J. D.; Fout, T.; Plasynski, S.; McIlvried, H.; Srivastava, R. D. *Int. J. Greenhouse Gas Control* **2008**, *2* (1), 9–20.
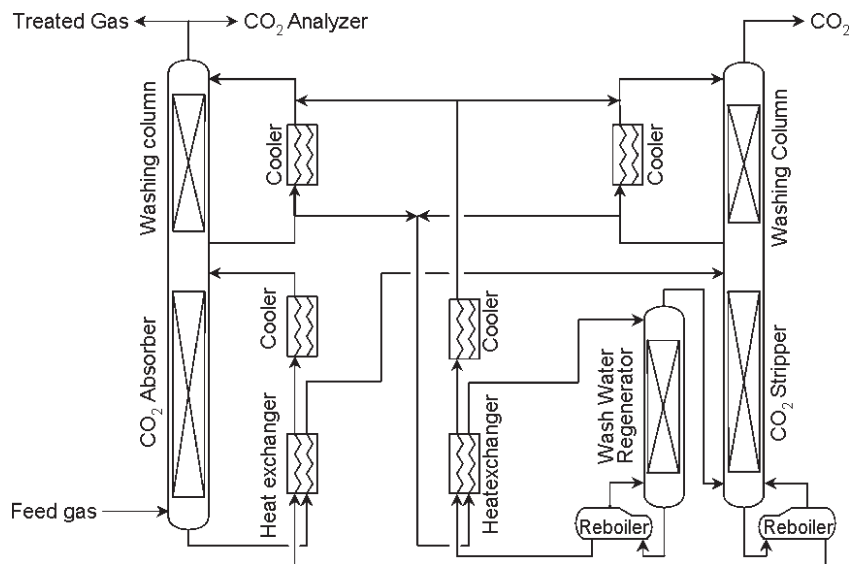
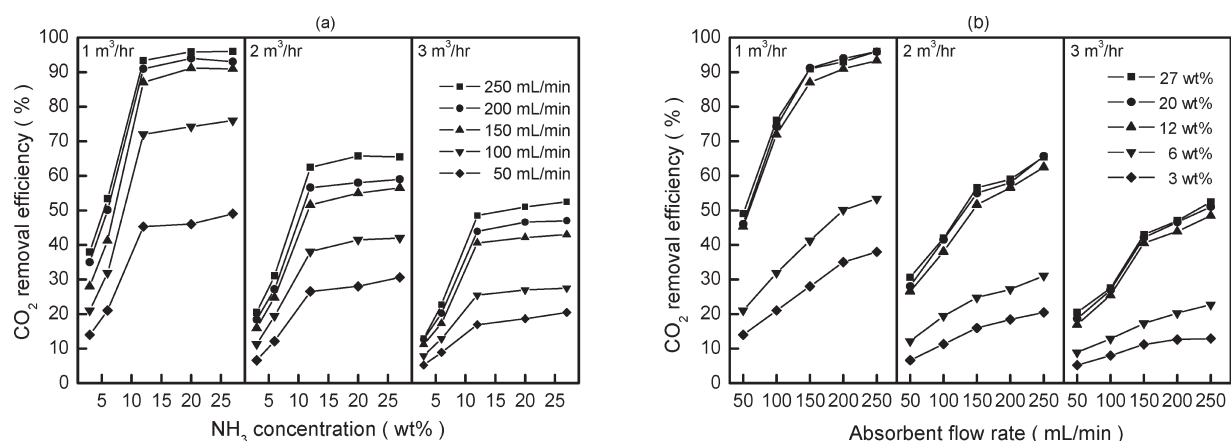**Figure 2.** Schematic diagram of a lab-scale continuous CO_2-capture apparatus.

Figure 3. Effect of the (a) NH_3 concentration and (b) absorbent flow rate on CO_2 removal efficiency. Feed gas flow rate, $1-3$ m^3/h; absorbent flow rate, $50-250$ mL/min; regeneration temperature, 85 °C.

removal efficiency is similar with NH_3 concentrations above 12 wt % and clearly different and lowered below this NH_3 concentration. The results of experiments under feed gas flow rates of 2 and 3 m^3/h reveal lowered removal efficiency than that at a feed rate of 1 m^3/h; however, the same tendency of the removal efficiency is observed at the same NH_3 concentration and absorbent flow rate as those of 1 m^3/h.

These results indicate that the removal efficiency depends upon the flow rate and is more dependent upon the NH_3 concentration, reflecting the general behavior of gas absorption in a liquid. This means that the NH_3 concentration higher than 12 wt % does not affect the removal efficiency. Therefore, the optimal NH_3 concentration is 12 wt %, as shown in Figure 3.

4.2. Effect of the Regeneration Temperature. To investigate the effect of the regeneration temperature, CO_2 removal efficiencies were measured under various reboiler temperatures and NH_3 concentrations. Figure 4 shows the removal efficiency under various regeneration temperatures.

As the regeneration temperature increases, the removal efficiency increases with a sigmoidal shape; it thereafter

(22) Fabrizio, M.; Maurizio, P.; Piero, S. *Green Chem.* **2006**, *1*, 995–1000.

shows a rapid increase to the maximum value and remains nearly constant. The temperatures at which CO_2 removal efficiency changes from a rapid increase to a steady value were 87 °C for 15 wt % NH_3, 90 °C for 12 wt % NH_3, 93 °C for 9 wt % NH_3, 95 °C for 6 wt % NH_3, and 97 °C for 3 wt % NH_3. This means that the temperature at which the removal efficiency reaches a nearly constant value is the optimal regeneration temperature and depends upon the NH_3 concentration. To operate the continuous system efficiently, the regeneration system should be operated at high temperature when the NH_3 concentration of the absorbent is low. Considering that the regeneration at higher than optimal temperature conditions causes energy loss, operation using an absorbent of low NH_3 concentration reduces CO_2 absorption capacity. The selection of an optimal NH_3 concentration and regeneration temperature is important for efficient operation. For the selection of these operating parameters, a theoretical approach is suggested in the following.

4.3. Effect of the Regeneration Temperature on CO_2 Loading of a Rich Absorbent. The effect of the regeneration temperature on CO_2 loading was investigated by measuring the amount of CO_2 dissolved in the absorbent. Figure 5 shows the CO_2 loadings for lean and rich absorbents.
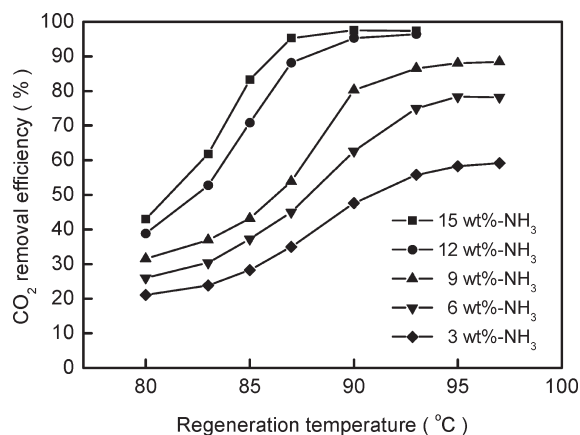
Figure 4. Effect of the regeneration temperature on CO_2 removal efficiency. Feed gas flow rate, 1 m^3/h; absorbent flow rate, 150 mL/min.

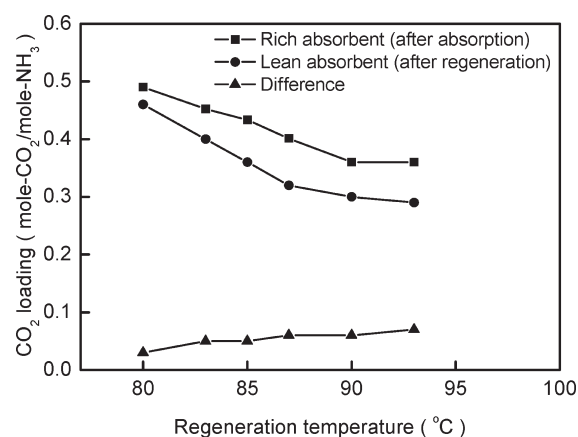**Figure 5.** CO_2 loadings for lean and rich absorbents under various regeneration temperatures. Feed gas flow rate, 1 m^3/h; absorbent flow rate, 150 mL/min; NH_3 concentration, 12 wt %.

As the regeneration temperature increases, CO_2 loadings for lean and rich absorbents decrease but the difference in CO_2 loading increases. These results agree well with those in Figure 4. At a regeneration temperature above 90 °C, the steady removal efficiency of 12 wt % NH_3 and CO_2 loading of absorbents are nearly constant. This means that regeneration at low temperature produces a lean absorbent, of which CO_2 loading is relatively high. Furthermore, it leads to a small CO_2 loading difference between lean and rich absorbents and, consequently, low removal efficiency. CO_2 loadings for rich absorbents with other NH_3 concentrations range from 0.35 to 0.38 and are listed in Table 1.

Through the continuous CO_2-capture experiments, it was found that the removal efficiency depends upon the operation parameters, such as regeneration temperature, NH_3 concentration, and CO_2 loadings for rich absorbents. A method to select the optimal operation parameters is theoretically studied in the following.

4.4. Theoretical Study To Select the Optimal Operation Parameters. Figure 6 shows the calculated mole fractions of CO_2 and NH_3 in the vapor phase at VLE of different CO_2 loadings and temperatures under atmospheric pressure. As the temperature increases, the mole fractions of CO_2 and NH_3 decrease and then remain steady above 95 °C. The steady-state mole fractions of CO_2 and NH_3 above this temperature can be explained by the evaporation of H_2O.

Table 1. Comparison of the Calculated Optimal Regeneration Temperature to Experimental Results

NH_3 concentration (wt %)	CO_2 loading[a] (mol of CO_2/mol of NH_3)	removal efficiency (%)	regeneration temperature	
			experiment[b] (°C)	calculation[c] (°C)
3	0.38	> 55	97	98
6	0.35	> 75	95	93
9	0.35	> 85	93	92
12	0.36	> 95	90	90
15	0.37	> 95	87	88

[a] CO_2 loading for rich absorbent. [b] The temperature where CO_2 removal efficiency changes from a rapid increase to a steady value in Figure 4. [c] The lowest temperature where the mole fraction of NH_3 in the vapor phase is higher than that of CO_2 at equilibrium.

Because the vapor pressure of H_2O is relatively small at low temperatures, the mole fractions of CO_2 and NH_3 are high and become steady when the vapor pressure of H_2O is relatively high at high temperatures. As shown in Figure 6a, the mole fraction of CO_2 in the vapor phase is higher than that of NH_3 until 84 °C. The temperature at which the mole fraction of CO_2 is higher than that of NH_3 increases as CO_2 loading increases. This temperature is 87 and 93 °C for CO_2 loading of 0.36 and 0.38, respectively, as shown in panels b and c of Figure 6. The calculation results show the same behavior when CO_2 loading is below 0.4, and the mole fraction of CO_2 is higher than that of NH_3 when CO_2 loading is above 0.4, regardless of the NH_3 concentration. In a continuous process, a rich absorbent is generated in the regeneration system. As the regeneration proceeds, the rich absorbent moves to the equilibrium state of the regeneration system. Therefore, it can be said that the regeneration depends upon the equilibrium state of the rich absorbent in the regeneration condition.

To correlate the results in Figure 6 with the behavior of regeneration, the reactions in Figure 1 are considered. The electrolyte reactions are known to be very complicated. and it is thus difficult to understand the overall behaviors of absorption and desorption simultaneously. Even though individual electrolyte reactions occur in a liquid phase, the reaction of CO_2 with aqueous NH_3 solution can be said to reversibly produce ammonium carbamate (NH_2COONH_4), ammonium carbonate (($NH_4)_2CO_3$), and ammonium bicarbonate (NH_4HCO_3) through the formation of bicarbonate (HCO_3^-) and ammonium ions (NH_4^+). For ease of understanding, the overall reversible reactions can be simplified as given in the following formulas:

$$NH_2COONH_4 \leftrightarrow 2NH_3 + CO_2 \qquad (7)$$

$$(NH_4)_2CO_3 \leftrightarrow 2NH_3 + CO_2 + H_2O \qquad (8)$$

$$NH_4HCO_3 \begin{matrix} \leftrightarrow NH_4^+ + HCO_3^- \\ \leftrightarrow NH_3 + CO_2 + H_2O \end{matrix} \qquad (9)$$

Stoichiometrically, 1 mol of ammonium carbamate or carbonate produces 2 mol of NH_3 and 1 mol of CO_2, whereas 1 mol of ammonium bicarbonate produces 1 mol of NH_3 and CO_2. As CO_2 absorption proceeds, the amount of ammonium bicarbonate increases through the reaction of ammonium carbamate and carbonate, which formed at low and medium CO_2 loading with additionally absorbed CO_2 at high CO_2 loading.[22] Considering the above reactions from the viewpoint of regeneration, the regeneration of a rich absorbent entails the decomposition of carbonated ammonia
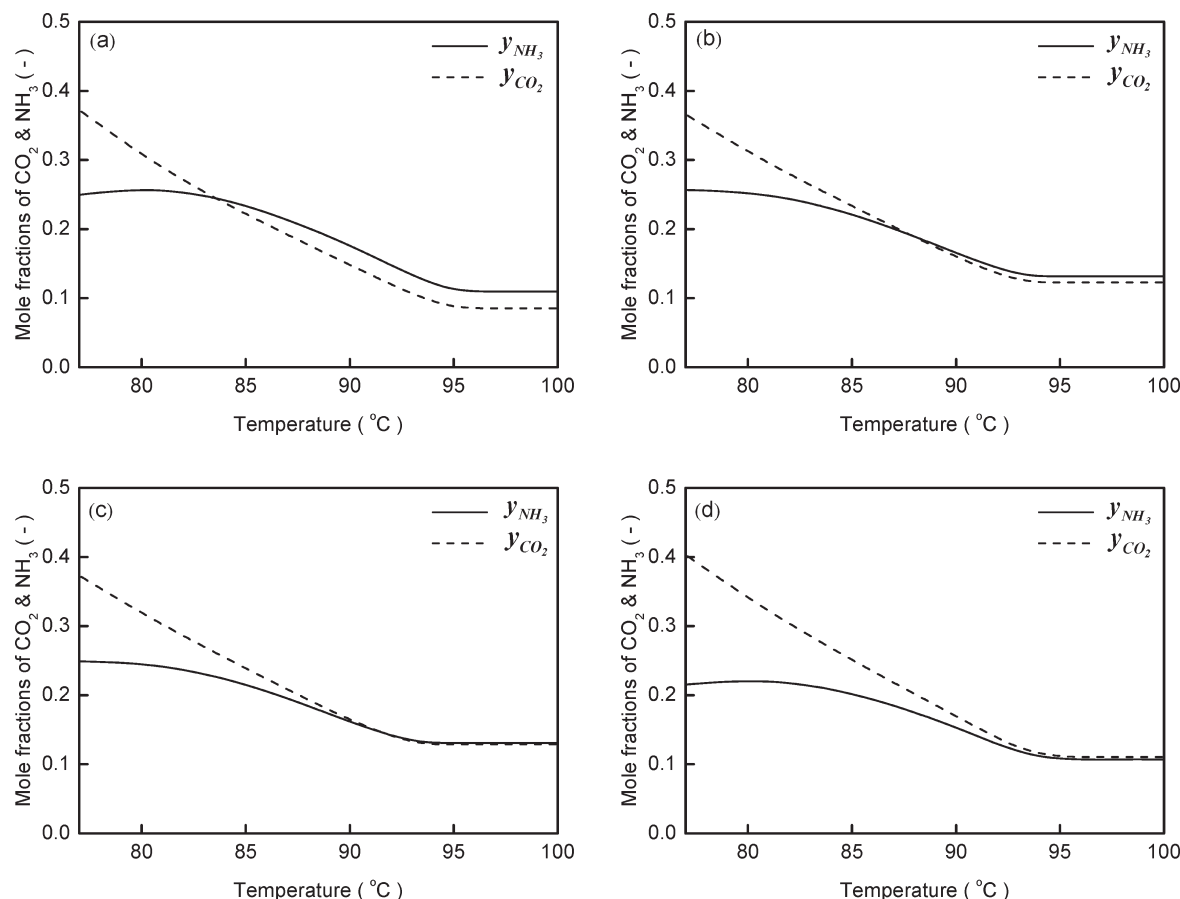
Figure 6. Calculated mole fractions of CO_2 and NH_3 in vapor phase at VLE under CO_2 loading of (a) 0.3, (b) 0.36, (c) 0.38, and (d) 0.4. NH_3 concentration, 12 wt %; property method, ElectrolyteNRTL; process model for VLE, flash.

to CO_2, NH_3, and H_2O. Because regeneration begins after absorption, ammonium bicarbonate that formed at high CO_2 loading is regenerated with the production of the same amount of NH_3 and CO_2, at which the mole ratio of NH_3/CO_2 in the vapor phase is approximately unity. In continuous operation, the produced NH_3 in the vapor phase is separated at the washing column installed above the CO_2 stripper and recovered from the wash water regenerator to the CO_2 stripper. Through the recovery of NH_3, the concentration of NH_3 in the rich absorbent is maintained at a constant level and the amount of NH_3 in the vapor phase becomes larger than that of CO_2. Therefore, the mole ratio of NH_3/CO_2 is larger than unity, and this also applies even in the case of regeneration with ammonium carbamate and carbonate. Although the amounts of carbonated ammonia species in the rich absorbent are difficult to quantify, the produced moles of NH_3 are at least larger than that of CO_2. Under proper regeneration of the rich absorbent, the mole ratio of NH_3/CO_2 in the vapor phase should be larger than unity.

On the basis of the above stoichiometric consideration, the preferred regeneration temperature can be inferred from the mole fractions of CO_2 and NH_3 in the vapor phase at equilibrium. As shown in Figure 6, the mole fractions of CO_2 and NH_3 cross over each other at different temperatures, which depend upon the CO_2 loading. The regeneration behavior is explained for two cases of temperature at VLE under constant CO_2 loading and pressure. In the case of the temperature at which the mole fraction of NH_3 in the vapor phase is larger than that of CO_2, the mole ratio of NH_3/CO_2 in the vapor phase at equilibrium is larger than unity. Because the

rich absorbent moves to the state of equilibrium at the regeneration condition, the mole ratio of NH_3/CO_2 will be the same as that for proper regeneration. On the other hand, the stoichiometrically preferred regeneration condition is not satisfied when the mole fraction of NH_3 in the vapor phase is smaller than that of CO_2. Therefore, the theoretical approach based on the VLE and simplified overall reactions of the CO_2–NH_3–H_2O system provides a means of estimating the proper regeneration temperature and CO_2 loading for a rich absorbent.

4.5. Comparison to Experimental Results. Through consideration of the mole fractions of CO_2 and NH_3 in the vapor phase at equilibrium, the regeneration temperatures at which the removal efficiency is nearly constant are compared to the calculated temperature at which the mole fraction of NH_3 is higher than that of CO_2 in the vapor phase at equilibrium under the same NH_3 concentrations and CO_2 loadings as employed in the experiments.

Table 1 represents a comparison of temperatures, where complete regeneration starts with the calculated values under the same conditions as used in the experiment. As shown in Figure 4, the removal efficiency increases rapidly and slows to near constant as the regeneration temperature increases. For simplicity, complete regeneration is defined such that it occurs at the temperature where the removal efficiency changes from a rapid increase to a steady value. The removal efficiency is proportionally increased from 55 to 95% as the NH_3 concentration increases from 3 to 15 wt %, but CO_2 loading of the rich absorbent is nearly the same, in a range from 0.35 to 0.38, regardless of the NH_3 concentration. The temperature of

complete regeneration increases as the NH_3 concentration increases, and the difference between the values obtained from the experiment and calculation is within ±2 °C. Therefore, the theoretical approach can be used for the selection of the regeneration temperature within the same accuracy.

4.6. Behaviors above the Regeneration Temperature. In addition to selection of the temperature where complete regeneration occurs, the steady removal efficiency above the regeneration temperature is also considered using the above approach. As shown in Figure 6, because the mole fractions of CO_2 and NH_3 are affected by the evaporation of H_2O above the regeneration temperature, the mole fraction of H_2O in the vapor phase should be considered.

As shown in Figure 6, when the temperature is above the regeneration temperature where the mole fraction of NH_3 in the vapor phase is higher than that of CO_2, the mole fractions of NH_3 and CO_2 decrease because of the evaporation of H_2O. Therefore, the regeneration behavior can be more accurately understood by considering the mole fraction of H_2O in the vapor phase. The regeneration critical condition is introduced and defined as the following formula:

$$\xi_{H_2O} = \frac{y_{NH_3} - y_{CO_2}}{y_{H_2O}} \qquad (10)$$

where ξ_{H_2O} is the regeneration critical condition including H_2O evaporation and y_{NH_3}, y_{CO_2}, and y_{H_2O} are mole fractions of NH_3, CO_2, and H_2O in the vapor phase at equilibrium, respectively.

Figure 7 shows the critical condition for regeneration under different CO_2 loadings and regeneration temperatures. When the CO_2 loading is 0.36 for 12 wt %, which is shown in Table 1, the regeneration critical condition increases from negative to zero at 90 °C and 0.01 at 94 °C and remains steady above this temperature. Comparing the removal efficiency in Figure 4, the dependency of the critical condition upon the temperature is in good agreement with the removal efficiency. The same results are obtained for other NH_3 concentrations. This indicates that the regeneration with a negative critical condition is incomplete and the regeneration with a critical condition above zero is complete. Because the regeneration is complete at high temperatures but consumes extra energy by the evaporation of H_2O, the degree of regeneration and energy loss should be optimized. For this purpose, the regeneration critical condition is a useful parameter for estimation of the optimal regeneration temperature.

4.7. Selection of the Optimal NH_3 Concentration. The calculation of the regeneration critical condition using mole fractions of CO_2, NH_3, and H_2O is applied to select the optimal NH_3 concentration.

Figure 8 shows the calculated regeneration critical condition under different NH_3 concentrations and CO_2 loadings. As the NH_3 concentration increases, the regeneration critical condition increases rapidly up to 9 wt % and the rate of increase then slows above this concentration, regardless of CO_2 loading. In general, higher removal efficiency can be achieved with a higher absorbent concentration, but use of a NH_3 concentration higher than a specific value does not increase the removal efficiency. In the present study, the experimental results shown in Figure 3a indicate that NH_3 concentrations above 12 wt % have little effect increasing the removal efficiency or the critical condition for regeneration. Although the dependency of the regeneration critical condition on the NH_3 concentration does not precisely agree with
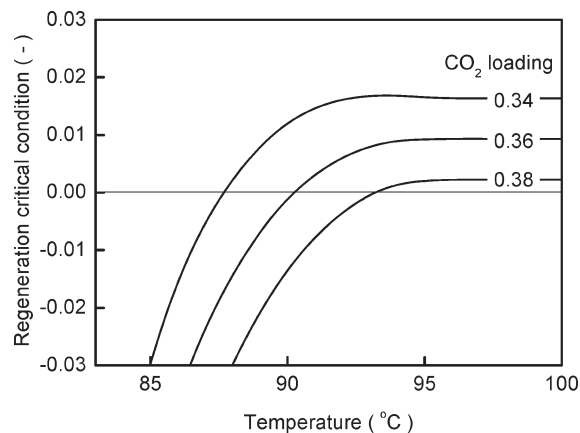

Figure 7. Calculated regeneration critical condition including evaporation of H_2O. NH_3 concentration, 12 wt %; property method, ElectrolyteNRTL; process model for VLE, flash.
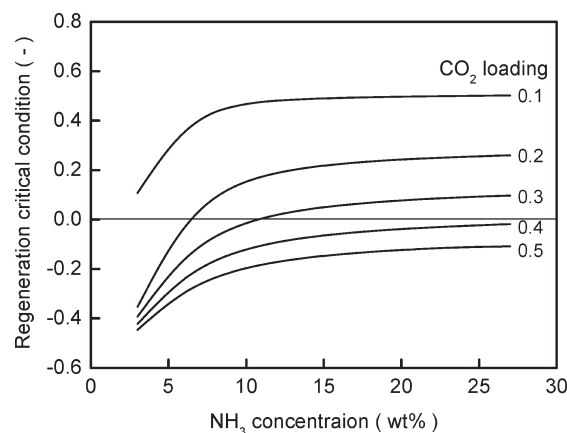

Figure 8. Calculated regeneration critical condition including evaporation of H_2O. Regeneration temperature, 85 °C; property method, ElectrolyteNRTL; process model for VLE, flash.

that of the removal efficiency in Figure 3a, the optimal NH_3 concentration for continuous operation can be estimated approximately by the regeneration critical condition.

5. Conclusions

The behaviors of a continuous CO_2-capture process can be understood through a comparison of operation results with the optimal parameters obtained using the calculated mole fractions of CO_2, NH_3, and H_2O in the vapor phase at equilibrium. On the basis of this comparison, the temperature where the mole fraction of NH_3 is higher than that of CO_2 in the vapor phase at equilibrium can be used for estimation of the proper regeneration temperature. The regeneration critical condition, which includes the evaporation of H_2O, is newly introduced. The behaviors above the estimated regeneration temperature could be understood, and the optimal NH_3 concentration could be estimated. Because the concentrations above 12 wt % had little effect on the removal efficiency, the optimal NH_3 concentration was suggested as 12 wt %. Additionally, it can be suggested that a rich absorbent easily regenerates when CO_2 loading is below 0.4, regardless of the NH_3 concentration.

The suggestions can be used as guidelines for the design and operation of CO_2 absorption−desorption using an aqueous NH_3 solution. The approaches derived from VLE in a CO_2−NH_3−H_2O system can be used to estimate the operating conditions of a regeneration system.